Engineering Structures 249 (2021) 113108

Contents lists available at ScienceDirect

Engineering Structures

journal homepage: www.elsevier.com/locate/engstruct

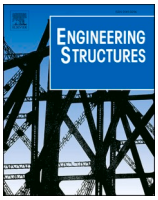

Optimal placement of viscous wall dampers in RC moment resisting frames using metaheuristic search methods

Ali Erdem Çerçevik [a,*], Özgür Avşar [b], Abdullah Dilsiz [c]

[a] Department of Civil Engineering, Bilecik Seyh Edebali University, Bilecik, Turkey
[b] Department of Civil Engineering, Eskisehir Technical University, Eskisehir, Turkey
[c] Department of Civil Engineering, Ankara Yıldırım Beyazıt University, Ankara, Turkey

ARTICLE INFO

Keywords:
Viscous wall dampers
Placement Optimization
Bat Algorithm (BA)
Dragonfly Algorithm (DA)

ABSTRACT

Viscous wall dampers (VWDs) are one of the most effective energy dissipation devices for the seismic performance enhancement of buildings. The number of VWDs as well as their positions in the building directly affects the seismic performance. In this study, two of the metaheuristic algorithms were employed for the optimal placement of VWDs in a reinforced concrete (RC) special moment resisting frame (SMRF) in order to achieve a safe yet cost effective solution. Bat algorithm (BA) and dragonfly algorithm (DA) were adopted to achieve the minimum number of VWDs by placing them in the most suitable positions of a 15 story RC SMRF. The floor accelerations and inter-story drift ratios (ISDRs) are considered as the constraints for the position optimization of VWDs with the objective of minimum number of VWDs. The application-programming interface (API) was employed for the interaction and data transfer between the structural analysis program ETABS and the Matlab program for optimization operations. Nonlinear response history analyses (NRHA) were conducted using recorded earthquake ground motions. Optimal placement for the minimum number of VWDs was achieved by using metaheuristic search algorithms. The additional damping provided by VWDs is effective in reducing the max ISDRs. However, higher damping ratios do not always result in the minimum floor accelerations. Therefore, an optimum damping ratio provided by VWDs needs to be sought for achieving minimum floor accelerations.

1. Introduction

Passive seismic control systems can protect the structures from dynamic effects by preventing structural damage and fulfill the performance requirements of safety of life and property. As the passive seismic control systems, viscous wall dampers (VWDs) are influential remedies for the enhancement of the seismic performance of buildings, since they effectively reduce the inter-story drifts and floor accelerations [1]. Inter-story drift ratios (ISDR) of buildings should be limited not only to prevent structural damage, but also to protect the non-structural components from seismic effects. In addition, lateral displacements caused by wind in such structures should be reduced to provide the comfort of residents. In order to reduce the lateral displacements, VWD was developed by Arima et al. in the late 1980 s [2]. VWDs increase the seismic resistance of the building by providing additional damping to the structure. Besides, VWDs do not intervene the building considerably as compared to other viscous dampers because of their similarity to a structural wall in architectural point of view. Although the use of VWDs has increased in different countries, researches related with their optimal placement in buildings by considering their structural response are scarce. This study addresses on the optimal placement of VWDs by considering the seismic response of RC SMRFs to minimize the number of required VWDs and hence provide a cost effective solution for RC SMRFs with VWDs.

A typical VWD is composed of two parts, where the first one is a steel tank fixed to the lower floor girder and filled with viscous liquid. The second part of the VWD is a vertical steel plate which is fixed to the upper-floor girder and placed in the tank and free to move in lateral direction along the viscous fluid in the tank (Fig. 1). As the structure makes relative displacement between the floors during lateral loading, the plate in the viscous liquid moves along the in-plane direction of the tank of VWD and provides additional damping to the structure. Although the amount of damping varies depending on the speed of the lateral movement, the total damping of the building increases with the effect of VWDs. As a result, the inter-story drift ratio and floor accelerations are reduced, and seismic damage in structural and non-structural

* Corresponding author.
E-mail addresses: erdem.cercevik@bilecik.edu.tr (A. Erdem Çerçevik), ozguravsar@eskisehir.edu.tr (Ö. Avşar), adilsiz@ybu.edu.tr (A. Dilsiz).

https://doi.org/10.1016/j.engstruct.2021.113108
Received 10 December 2020; Received in revised form 20 July 2021; Accepted 28 August 2021
Available online 9 October 2021

components is minimized with the additional damping supplied by VWDs.

Earlier studies reporting the results of the research on VWDs were on steel moment frame systems [2], and presented the test results of full-scale structural specimens with and without VWDs on the shake table. The test results indicated a 2/3 reduction in relative displacements and approximately 50% reduction in floor accelerations at the roof compared to the conventional moment frame. Recently, VWD devices were tested at the University of California, San Diego to identify the characteristic features of the VWDs and define the corresponding modeling parameters to establish expected seismic performance of a hospital building which would be constructed in highly seismic region [3]. The full-scale prototype specimens of these tests were selected to represent variable values of displacements and velocities in different loading conditions according to ASCE 7–05 [4]. Based on the test results, VWD force–displacement relations were identified as illustrated in Fig. 2, with the indicative parameters, i.e. force at zero displacement (F_0), effective stiffness (K_{eff}), force at maximum device displacement (F @ D_{max}), and the area of hysteresis loop (E_{loop}). The hospital building was designed and built in San Francisco, CA, US according to these test results [3].

An experimental study was conducted by testing 3-story RC buildings with and without VWDs on shaking table [5]. According to the experimental findings, which are also verified by the finite element analysis results, the damping ratio of the RC building with VWDs was 20% larger and its displacements decreased by 30 to 60% compared to the RC building without VWDs. In a similar study, a 3-storey ¼ scaled steel space frame with a VWD was tested by [6]. It has been demonstrated that VWDs greatly increase the natural frequencies and decrease inter-storey shear forces and acceleration values. Based on these experimental studies a finite element model of a 3D nonlinear VWDs was also proposed [7].

Recently, seismic performance of a prototype reinforced concrete (RC) special moment resisting frame (SMRF) with VWDs located in a seismic area in Turkey was investigated analytically [1]. The seismic performance of the 15-story building with an enriched design using VWDs was compared with the performance of a conventional SMRF system. Nonlinear response history analyses (NRHA) were conducted on the RC SMRF with and without VWDs. In the study, first two different design configurations were considered for the placement of VWDs in the spans of RC SMRF, and it was concluded that when the VWDs are placed in the lower floors a better structural performance was obtained. Then, following this preliminary conclusion, a number of VWD configurations were tried with the aim of satisfying the target peak inter-story drift values. This study clearly demonstrated the importance of optimum placement of VWDs in building spans for achieving target structural performance parameters with minimum number of VWDs. Although there are several optimization studies on other types of dampers, there is no study on the optimum placement of VWDs to achieve minimum number of VWDs in previous studies.

Many different methods such as cone programming approach, transfer functions, combined fitness function, velocity-depended damper quantities approach and sequential quadratic programming method have been employed in the position optimization studies of the dampers employed in structures [8–14]. In these studies, the placement of dampers was generally optimized by taking the structural performance parameters into account. Stochastic optimization of dampers was conducted by [15,16] to consider the uncertainties of seismic excitations. In addition, there are several studies of optimum damper placement using gradient methods [17,18]. However, non-gradient methods including metaheuristic algorithms are used successfully in structural optimization problems [19–21]. Non-gradient methods can find optimum results better than gradient methods, advantages to their ability to solve general engineering problems [22].

Recently, metaheuristic algorithms have been used to determine the optimum placement of dampers, similar to these studies. The metaheuristic algorithms used include the artificial bee colony algorithm [23], differential evolution algorithm [24], genetic algorithm [25,26], firefly algorithm [27]. Although there are plenty number of optimization studies for the placement of dampers in the literature, there is no study in relation with the optimization of VWD placement in buildings considering their structural performance.

This study focuses on the use of metaheuristics algorithms to designate the optimum VWD placement in RC SMRF systems by constraining the structural response in terms of certain limitations on floor accelerations and inter-story drift ratios. On the purpose, an optimization program has been developed using the bat algorithm (BA) [28] and the dragonfly algorithm (DA) [29] to determine the optimum span locations of VWDs for a 15-storey RC SMRF building model. The reason for choosing these two algorithms (BA and DA) is that they are relatively new algorithms and show strong results in constrained optimization problems. In addition, BA and DA can find satisfactory results in the solution of many binary problems, where binary variables are considered in this study [30–35]. While limiting the structural responses, it is also aimed to minimize the number of VWDs and hence cost, as well. Structural analyses of the example building were performed by ETABS software [36]. The application-programming interface (API) was implemented to provide data transfer and interaction between the optimization algorithms and structural analysis software. By the application of the proposed optimization procedure, VWD placement in RC SMRF was optimized with minimum number of required VWDs that fulfill the specified building performance limits. Finally, the seismic performance of RC SMRF for three cases; (i) RC SMRF with optimized VWD placement, (ii) RC SMRF without VWD, and (iii) RC SMRF with VWD in all possible spans, were compared to highlight the necessity of the proposed optimization method not only for a cost effective design but also to achieve the most favorable structural response with VWDs.

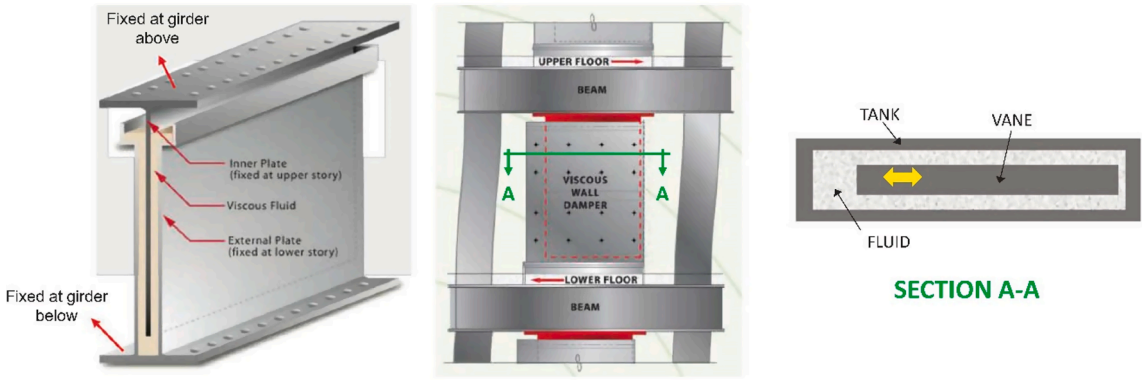

Fig. 1. The details of VWD and its components [1].

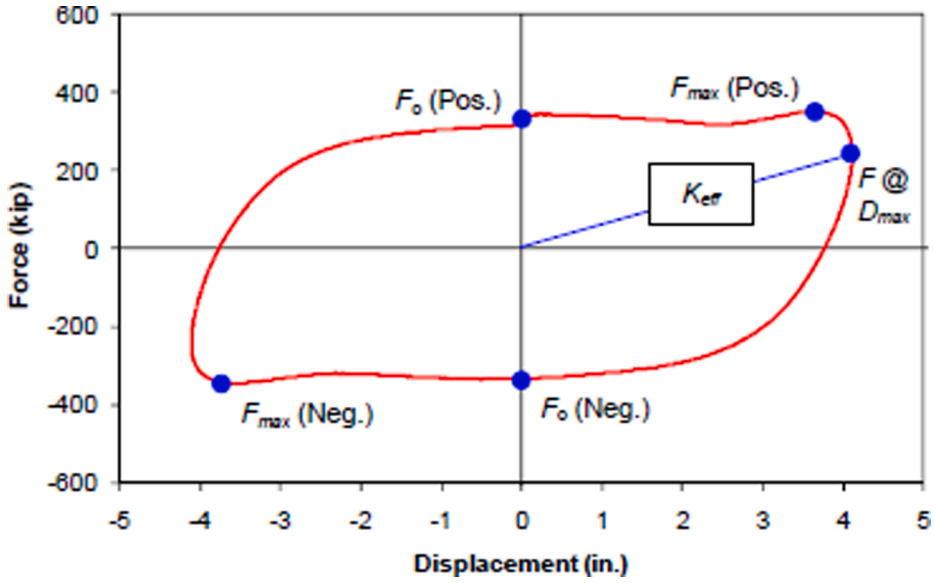

Fig. 2. VWD force–displacement relation [3].

2. Problem formulation for position optimization of viscous wall dampers

The procedure applied for the position optimization problem of VWDs in this study, is explained in this section. The objective function (f) is specified to find the minimum number of VWDs in the most appropriate spans of the RC SMRF,

$$f = \sum(w) f_{penalty} \tag{1}$$

while satisfying the following constraints:

$$a_{\max} \le a_{limit} \tag{2}$$

$$s_{\max} \le s_{limit} \tag{3}$$

In Eqs. (1)-(3), w is the number of VWDs, $a_{\max}$ and a_{limit} represent the calculated peak floor acceleration (for all 15 floors) and its corresponding limit, respectively. $s_{\max}$ and s_{limit} represent the calculated peak inter-story drift ratio (for all 15 stories) and corresponding drift limits, respectively. $f_{penalty}$ penalty function as formulated by Eqs. (4a, 4b).

$$f_{penalty} = \begin{cases} \left(1 + \kappa_1 \cdot \dfrac{a_{\max}}{a_{limit}}\right)^{\kappa_2}, a_{limit} < a_{\max} \\ 1.0, a_{limit} \ge a_{\max} \end{cases} \tag{4a}$$

$$f_{penalty} = \begin{cases} \left(1 + \kappa_1 \cdot \dfrac{s_{\max}}{s_{limit}}\right)^{\kappa_2}, s_{limit} < s_{\max} \\ 1.0, s_{limit} \ge s_{\max} \end{cases} \tag{4b}$$

In Eqs. (4a, 4b), if $a_{\max}$ or $s_{\max}$ exceed the specified limits by constraints, the penalty function f is specified by the given equations. By this way, whenever infeasible VWD placements are generated for which the calculated VWD positions exceeding the specified peak floor acceleration or peak inter-story drift ratio limits, they are seriously penalized to direct the optimization algorithm towards feasible regions of the search space. A formerly proposed penalty function term [23] is adopted in the present study. The values of 1 and 2 can be used for the constants κ_1 and κ_2 in Eqs. (4a, 4b), respectively [37].

3. Optimization methods employed

VWDs are usually placed in all possible spans of story levels where inter-story drift ratios (ISDR) are high or at lower story levels according to the conventional design. Since a VWD equipment placed in any span can change the structural response considerably, such a random placement approach may cause overuse of VWDs and/or result in unfavorable structural performance. If VWDs are placed in the most appropriate spans, the desired performance level in the structure can be achieved with the least number of VWDs. Design iterations applied by an experienced structural engineer might approximate the optimum design faster, however, the analyses and evaluation processes would still overwhelm the engineer as well as the computer systems. There are countless possibilities for the amount of VWD and possible placement spans. Thus, a fairly powerful solution is needed to place the minimum number of VWDs at the optimum spans that will provide the desired structural performance in countless possibilities. In this study, two recent metaheuristic search algorithms, namely bat algorithm (BA) [28] and dragonfly algorithm (DA) [29] were investigated in terms of their applicability and success in finding the optimum placement of VWDs. Brief explanations of BA and DA are presented in the following subsections.

3.1. Bat algorithm (BA)

Bat Algorithm (BA) is a swarm intelligence algorithm proposed in 2010 [28], which was inspired by the hunting behaviour of microbats. Microbats emit loud blows that are decisive for their approach to its target when searching for their prey in the dark. This behavior is called “echolocation”, so they can determine the location of their prey, as well as their distance and size.

While developing the mathematical model of BA, hunting of bats is considered with their echolocation ability based on 3 basic rules. Firstly, all bats use echolocation to distinguish prey and obstacles to detect the distance in-between. Secondly, all bats fly randomly and their track is characterized by their internal encoded position in space (x), frequency (f), and velocity (v). These three variables are updated at each iteration of the algorithm as follows;

$$f_i = f_{min} + (f_{max} - f_{min})\beta \tag{5}$$

$$v_i^t = v_i^{t-1} + (x_i^t - x_*) f_i \tag{6}$$

$$x_i^t = x_i^{t-1} + v_i^t \tag{7}$$

where x_i^t represents the new solutions and v_i^t is the velocities at time step t. Here x_* is the current global best solution that is located after

comparing all the solutions among all the n bats at each iteration t. $\beta \in [0, 1]$ is a random vector drawn from a uniform distribution. $f_{min} = 0$ and $f_{max} = 100$ are used, depending on the domain size of the problem of interest. Initially, each bat is randomly assigned a frequency value that is drawn uniformly from f_{min} to f_{max}.

The echolocation that the bats use to detect their prey is updated with the sound intensity and signal propagation rates they produce throughout iterations as the best solution is approached. As the bat approaches the hunt, it will decrease its loudness (A_i) and increase its rate of the pulse emission (r_i) as follows:

$$A_i^{t+1} = aA_i^t \tag{8}$$

$$r_i^{t+1} = r_i^0(1 - e^{-\gamma t}) \tag{9}$$

where α and γ are constants. $0 < a < 1$ and $\gamma > 0$ in the case it is found with the following:

$$A_i^t \to 0, r_i^t \to r_i^0, t \to \infty \tag{10}$$

Additionally, the bat will perform a local search by using uniform random walks to improve its position in space,

$$x_{new} = x_{old} + \varepsilon A^t \tag{11}$$

where $\varepsilon \in [-1, 1]$ is a random number and while A^t is the average loudness of all the bats at this time step.

BA also performs exploration and exploitation movements using loudness and pulse emission, similar to other swarm intelligence algorithms. BA can solve different problems with these random walk movements.

BA has been successfully applied to nonlinear engineering problems in the literature, such as structural optimization [38], traveling salesman problems [39], robotics and path planning [40] and planning the sports training sessions [41] selected from many others. Besides, a modified version of BA was formulated and implemented for the optimization of skeletal structures [42].

3.2. Dragonfly algorithm (DA)

Nature-based dragonfly algorithm (DA) was developed for the solution of single and multi-mode optimization problems [29]. The main inspiration of the DA originates from static and dynamic swarming behaviors. These two swarming behaviors are very similar to the following two main phases of optimization using metaheuristics: exploration and exploitation. Dragonfly flies in the static swarm (exploration) form small groups and move back and forth to find their prey. The main characteristic feature of the static dragonfly swarm is local movements and sudden changes in the flight path. Dynamic dragonflies (exploitation), are based on the collection of a large number of dragonflies and their migration to remote areas together.

The main purpose of the dragonfly herd is to survive. Therefore, it is necessary to escape from enemies and find food. To apply these two main objectives, there are five main parameters in the position updating of individuals in swarms. These five factors include control separation, alignment, cohesion, attraction (towards food sources), and distraction (towards outward enemies) of individuals in the swarm. Each of these behaviors is mathematically modeled as follows [29]:

The separation of the *i-th* dragonfly is calculated by Eq. (12);

$$S_i = -\sum_{j=1}^{N}(X - X_j) \tag{12}$$

where N is the number of neighboring individuals, X is the position of the current individual and X_j shows the position j^{th} neighboring individual. Alignment is calculated by Eq. (13);

$$A_i = \frac{\sum_{j=1}^{N} V_J}{\mathrm{N}} \tag{13}$$

where V_J shows the velocity of the j^{th} neighboring individual. The cohesion is calculated by Eq. (14);

$$C_i = \frac{\sum_{j=1}^{N} X_J}{\mathrm{N}} - X \tag{14}$$

Attraction towards a food source is calculated as follows;

$$F_i = X^+ + X \tag{15}$$

where X^+ is the position of the food source. Distraction towards an enemy is calculated by Eq. (16);

$$E_i = X^- + X \tag{16}$$

where X^- is the position of the enemy. It is assumed that the behavior of dragonflies is a combination of these five corrective patterns. To update the position of dragonflies in a search space and simulate their movements, two vectors are considered; namely position (X) and step (ΔX). The step vector can be considered as a velocity vector, and the direction of movement of dragonflies is given in Eq. (17);

$$\Delta X_{t+1} = (sS_i + aA_i + cC_i + fF_i + eE_i) + w\Delta X_t \tag{17}$$

where w is the inertia weight, t is the iteration counter, s shows the separation weight, a is the alignment weight, c indicates the cohesion weight, f is the food factor, and e is the enemy factor. The positions are calculated by Eq.18;

$$X_{t+1} = X_t + \Delta X_t \tag{18}$$

where t indicates the current iteration. As given in Eq. 19–21, levy flight is used to randomly determine the position of the dragonflies.

$$X_{t+1} = \acute{L}evy(d) \times X_t \tag{19}$$

$$\acute{L}evy(d) = 0.01 \times \frac{r_1 \times \sigma}{|r_2|^{\frac{1}{\beta}}} \tag{20}$$

$$\sigma = \left(\frac{\Gamma(1+\beta) \times \sin\left(\frac{\pi\beta}{2}\right)}{\Gamma\left(\frac{1+\beta}{2}\right) \times \beta \times 2^{\left(\frac{\beta-1}{2}\right)}} \right)^{1/\beta} \tag{21}$$

where $\Gamma(x) = (x-1)!$, d is the dimension of the position vectors, t is the current iteration, r_1 and r_2 are two random numbers in $[0,1]$ and β is a constant (equal to 1.5). The step of each dragonfly and position are updated in each iteration using Eqs. 19–21.

DA has found some applications in the literature. A modified version of DA was employed for optimization of frame structures [43]. The method has also been applied to different engineering optimization problems such as structural design optimization of vehicle components [44], feature selection [45] and optimization of orthotropic infinite plates [46].

4. Development of design optimization algorithms

The design optimization algorithms were developed in Matlab by integrating the two metaheuristic search algorithms with ETABS structural analysis software [36] in order to achieve position optimization of VWDs in RC SMRF system. Structural analyses of the investigated RC SMRFs were performed by virtue of ETABS software, for which the open application-programming interface (API) was implemented to provide data transfer and interaction between the optimization algorithms and structural analysis software. In Fig. 3., a general flowchart of the optimization algorithms developed with two metaheuristic search methods (BA, DA) is presented to solve the predefined problem.

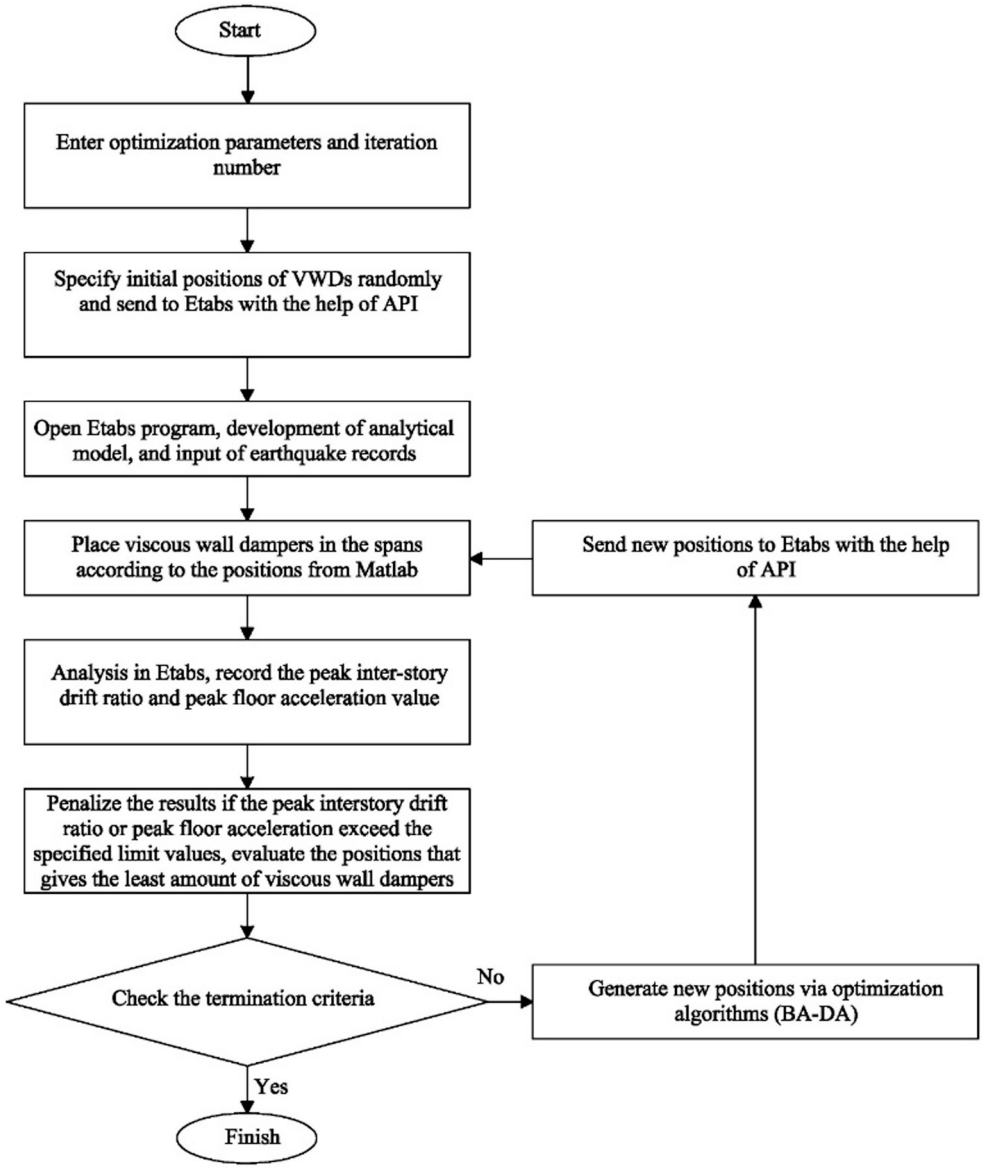

Fig. 3. A general flowchart of the optimization algorithms developed with BA and DA for the position optimization of VWDs.

4.1. ETABS API Implementation

ETABS's application programming interface is a tool for creating models, analyzing, adding-removing elements that provides the repetitive analysis required by the optimization process. It also allows to link ETABS with third-party tools, providing a way to exchange two-way model information with other programs. The VWD, which is the subject of work with API, can be placed in structural spans, removed or the analysis results can be recalled [36]. These features of API enabled to obtain repetitive solutions by the codes developed for the position optimization of VWDs.

4.2. Position optimization parameters

Two engineering demand parameters, i.e. ISDR (s_{limit}) and floor acceleration (a_{limit}), were considered as the limiting parameters in the proposed position optimization method for VWDs, as explained in previous sections. ISDR of buildings should be limited not only to prevent structural damage, but also to protect the non-structural components from seismic effects. Besides, floor accelerations can play a critical role for the safety of building contents and comfort of the residents. ISDR is limited in the high-rise building design in current Turkish Building Seismic Code TBSC (2018) [47] and these code limitations were adopted in this study as well. According to TBSC (2018), the average ISDR value of 11 ground motions should be less than 3% and the peak ISDR value should be less than 4.5%. Since the ISDR is limited by both the mean and peak demands, the ground motions that result the mean and peak ISDRs are selected accordingly, as explained in the next sections.

The peak floor acceleration limit has been selected as 10 m/s^2 based on the findings of the previous studies [48–50]. The floor accelerations have to be limited depending on the type of building and the purpose of use, but there are different approaches in literature. In this study, since a RC high-rise prototype building is handled and a minimum number of VWDs is sought according to the building characteristics, the peak floor acceleration limit is selected to be 10 m/s^2, after performing preliminary studies. However, it is always possible to perform position optimization for VWDs in accordance with the peak ISDR and floor acceleration limits suitable for the investigated structure type with the proposed optimization method.

While carrying out the optimization analyses, three runs were performed with each of the two optimization algorithms of BA and DA. The best solution of an algorithm in these runs, i.e. the one leading to the

minimum VWD number, was considered for the solution of the algorithm in that particular run. In all optimization cases, the population size was set to 25 and the maximum number of iterations was limited to 100 while running the two metaheuristic optimization algorithms. It was found that the 100 iterations were adequate for BA and DA to exhibit satisfactory convergence characteristics for the problem of interest.

5. Numerical example

5.1. Analytical model of the building

A 15-storey RC SMRF model was chosen for conducting the position optimization of VWD to achieve the minimum number of required VWDs. The building model was adopted from the previous study [1], in which the VWDs were placed based on trial and error approach without performing any optimization algorithm. The modeling details of VWD were applied as given in the modeling guide provided by the manufacturer [51], and used in previous study [1]. 3D view of the building model as well as its plan and elevation views (elevation view includes the basement stories under the main tower building only for simplicity and basement beams were not shown on the elevation view to distinguish the basement stories with the ground and normal stories) with the geometrical dimensions are shown in Fig. 4. RC SMRF building model has a symmetrical floor plan with 4x4 bays. The building model has 15 stories plus three basement stories, which have larger footprint areas compared to the stories above. These basements are surrounded by rigid basement structural walls, as shown in Fig. 4(a).

5.2. Structural system parameters

For the building model shown in Fig. 4, the story height, the dimensions of the structural members and the design loadings in gravitational direction are summarized in Table 1. The three-dimensional (3D) finite element model of the building studied was developed using ETABS software [36].

The beam and columns were modeled using 1D line elements, while the floor slabs and shear walls of the basement were modeled using 2D shell elements in the analytical model. Rigid beam-column joint assumption is adopted. The material properties of the RC structural system were defined using a constant concrete class of C50 with a 50 MPa nominal compression strength and reinforcing steel of Grade 420 with a 420 MPa yield strength. Nonlinearity was not considered for slab modeling and they were modeled as linear elastic plate elements. RC beam and column members, on the other hand, were modelled with line elements having nonlinear plastic hinges at member ends, which were defined according to TBSC [47] provisions using nonlinear material characteristics of concrete and steel. For the inherent damping modeling of the RC system, a uniform damping ratio of 2.5% was employed for all modes in accordance to TBSC provisions. Fast nonlinear analysis method was adopted with 20 Ritz modes for conducting NRHA. The model validation of the investigated building as well as the applicability of fast nonlinear analysis method for the developed analytical model was substantiated in the previous study [1].

5.3. Modeling of viscous wall damper (VWD)

The seismic performance of the buildings is highly interconnected with the position and number of VWDs in addition to their mechanical properties. Studies have shown how VWDs with different mechanical properties affect the structural responses [2,5–7]. In this study, as the main objective, the optimum placement of VWDs in RC SMRF was investigated to minimize the number of required VWDs by satisfying the target structural response. Therefore, the mechanical properties of the VWDs used in the study were kept constant, which were adopted from the results of the experimental tests [3] and suggested by the guide of the manufacturer [51].

Nonlinear link elements (NLLINK) were employed in ETABS to model the VWDs. The schematic representation of the analytical model of the building with VWDs is shown in Fig. 5. This nonlinear link element is basically a linear spring with a spring constant of K, which is connected in series with a damper modelled by "Exponential Maxwell Damper" characterized by C and α. The NLLINK is also shown in Fig. 5. The available double vane of 2.74 m tall and 2.13 m wide VWD was selected from the guide [51] and used in the study, since the story height above the basement is 3.6 m. The nominal mechanical properties of this type of VWDs are given as; $K = 71800$ kN/m, $C = 3015$ kN$\times$(sec/m)$^{\alpha}$, and $\alpha = 0.5$ [51]. The guide [51] also suggests the upper- and lower-bound property modification factors (λ) for different design approaches. In order to get the unfavorable maximum force demands the upper-bound factors are needed. The lower-bound factors, on the other hand, are used to obtain maximum displacement and drift demands. In line with the basic engineering demand parameter of ISDR in this study, the lower-bound modification factor of "$\lambda = 0.80$" was used. For the sake of conformity, these mentioned values were selected for the design parameters, which were also considered in the previous study [1].

The VWDs were modelled with two rigid vertical line elements centered in the bays together with NLLINK element that connects the ends of the rigid members at the story mid-height. Therefore, the hysteretic behavior of the VWD is lumped at this NLLINK [52]. Vertical rigid elements were connected to the horizontal rigid elements having a length equal to the half of the VWD width.

5.4. Implementation of the proposed optimization method to the numerical example

In order to determine the optimum number and distribution of the VWDs, the analyses were conducted in one direction only. The main reason for the uni-directional analysis is to save computation time when the numerous number of analyses considered during the optimization process in searching the optimum position of VWDs. Therefore, VWDs were placed in only two opposite outer faces of the building model in a symmetrical arrangement. This simplified approach is acceptable because the prototype building has a symmetric plan and does not have any irregularity in the plan and elevation. In each trial during the optimization process, VWDs were placed in the same spans only on two opposite outer facades not to induce any torsional irregularity in the structural system. In Fig. 6, the 3-D analytical model of the building developed in ETABS with VWDs placed in all spans of two outer facades of the building that are parallel to the earthquake excitation direction is shown.

As seen in Fig. 6, there are 60 possible spans on one side of the building in the 15-floor and 4-bay building model. This means that there are 2^{60} possibilities that should be considered in achieving the optimal positions of VWDs in this building. For VWD placement only the bays of the ground story and upper stories are considered, and those in the basement stories, which are surrounded by rigid basement structural walls are not included in the possibilities of VWD placement. It is quite a laborious process to find out how many of the spans and which of them would be used for placement of VWDs by satisfying the specified seismic response limits. The search for the optimum position of VWDs is made by using both bat and dragonfly metaheuristic optimization algorithms separately. For the building model aiming for optimum placement with the minimum number of VWDs in the 15-storey building, the binary versions of bat and dragonfly metaheuristic optimization algorithms were used. Running an optimization process in binary means an algorithm with only 0 and 1 variables without rational numbers. For this reason, it has been deemed appropriate to use metaheuristic optimization algorithms for the position optimization of VWDs in a 15-storey structure operating on a dual base. The optimization variable is the presence of VWDs in the investigated span; where "0″ indicates that there is no VWD in the investigated building span, while "1" indicates that VWD is present.

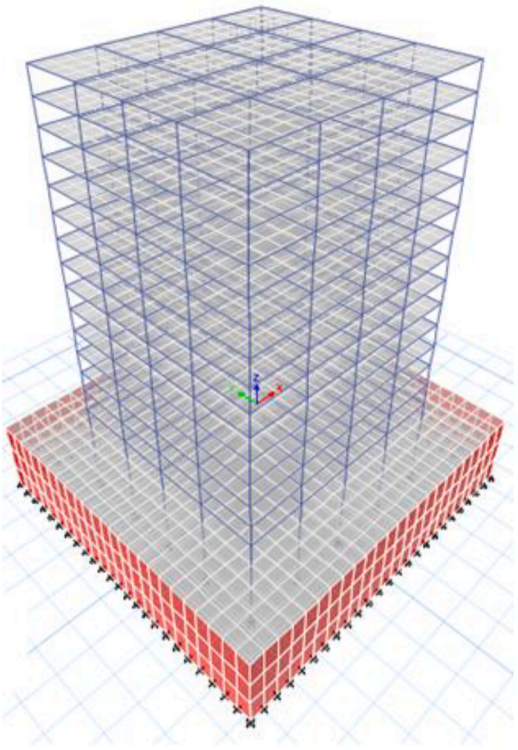

(a)

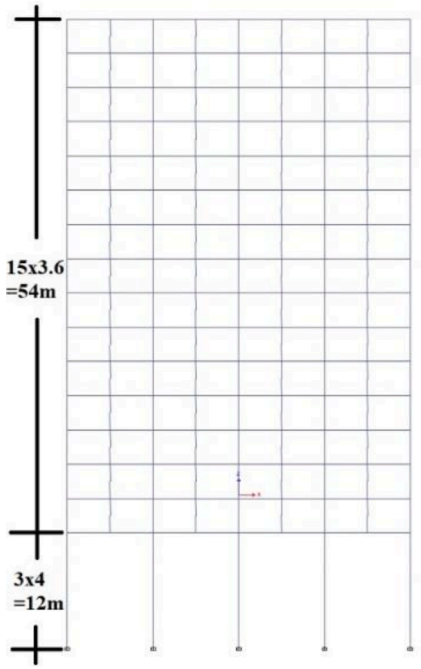

(b)

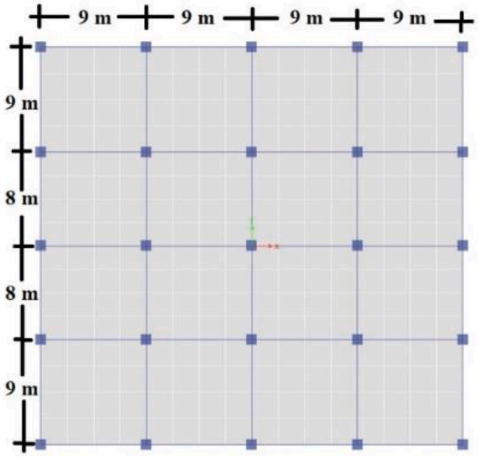

(c)

Fig. 4. (a) General 3D view of the building model, (b) Elevation view and (c) plan view of the building (dimensions are given in meters).

Table 1
Modeling details for dimensions and geometry of the building [1].

Stories	Basement	S1-S3	S4-S15
Story height (m)	4.0	3.6	3.6
Columns (m)	1.0*1.0	0.9*0.9	0.8*0.8
Beams (m)		0.8*0.6	
Slab thickness (m)	0.35	0.21	0.21
Dead Load (kN/m^2)	2.0	3.5	
Live Load (kN/m^2)	5.0	2.0	

6. Earthquake ground motion records

A minimum of eleven ground motion records shall be employed in NRHA as per TBSC [47]. Therefore, eleven ground motion records were selected and scaled with respect to the requirements of TBSC in the NRHA conducted for the optimization process. According to the code, at most three ground motion records can be selected from a single earthquake event. Moreover, the mean response spectrum of the selected ground motion records shall not be less than the code specified design spectrum for the period ranges between $0.2{\cdot}T_p$ and $1.5{\cdot}T_p$, where T_p is the fundamental natural period of the investigated building. The ground motion pairs were selected from the database of the Pacific Earthquake Engineering Research Center [53], and scaled accordingly. The selected records are given in Table 2.

The response spectra of the selected ground motion records were scaled matching with the target acceleration design spectrum defined for the site of the building. In Fig. 7, the scaled response spectra of the ground motions are presented in comparison with the code based design spectrum. As the site of the building, a specific location in İstanbul was selected with latitude of 41.084983° N and longitude of 29.006575° E. The maximum credible earthquake (MCE) level as per the current seismic code [47] was considered for the code based design spectrum. The building model was developed in ETABS without VWDs and modal analysis was performed to obtain T_p, which is determined as 3.55 s. The average spectral acceleration values of ground motion records scaled are greater than the design spectrum according to TBSC between 0.71 s ($0.2{\cdot}T_p$) and 5.33 s ($1.5{\cdot}T_p$) as shown in Fig. 7(b).

6.1. The effect of additional damping supplied by VWDs on displacement and spectral acceleration response of the building

Like the other types of energy dissipation systems, one of the main objective of using VWDs is to supply additional damping to the structural system. The variations of spectral accelerations and displacements of the selected 11 ground motions with respect to damping ratio are presented in Fig. 8 for $T_p = 3.55$ s. As the damping ratio increases, the spectral displacements reduce, while the trend is not the same for the spectral accelerations. Depending on the ground motion characteristics, spectral accelerations reduce up to a certain level of damping, after which the spectral accelerations increase as the damping increases (Fig. 8a). This was also emphasized in literature [55,56], such that for a certain vibration period, there is a certain damping ratio, which yields a local minimum in the acceleration response spectrum depending on the characteristics of the ground motion. In order to make a consistent comparison, the spectral values of various damping ratios are normalized with respect to the spectral value for 5% damping ratio for both spectral acceleration and displacement in Fig. 9. The mean of the normalized spectral displacement, on the other hand, has a consistent decreasing trend as the damping ratio increases as shown in Fig. 10b. This indicates that additional damping ratio is always beneficial for limiting drift demands, but after a certain value of damping ratio, spectral accelerations increase (Fig. 10a). This result also highlights the necessity of the optimization process to identify the critical damping ratio that results the local minimum spectral accelerations. In other words, high damping ratio does not guarantee a reduction in the floor accelerations, which can be searched through an optimization process.

6.2. Selection of critical EQ ground motions for optimization

The ground motion set containing 11 records presented in Fig. 7 was used for position optimization of VWDs in RC SMRF building. However, for the sake of brevity considering the analysis and processing time, rather than including all 11 ground motions in the optimization process,

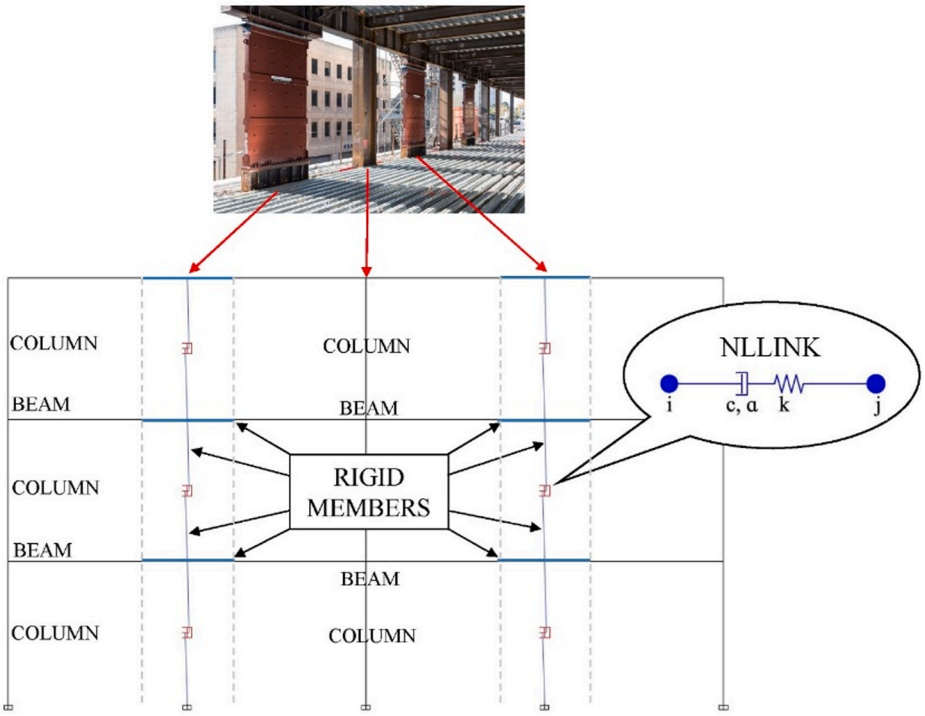

Fig. 5. Schematic representation of analytical model with VWDs.

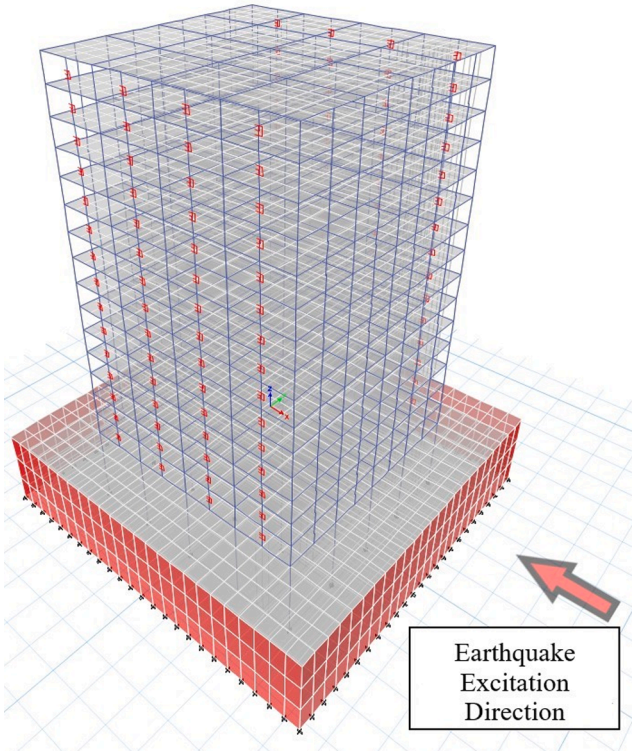

Fig. 6. Building model with VWDs placed in all spans (in this case) of two outer facades of the building in earthquake excitation direction.

analyses were performed with two of them which are determined as the most critical. Once the optimization process finalized, the optimum results were evaluated by conducting NRHA using the selected and scaled 11 ground motions. Initially, the NRHA were performed with 11 ground motions without VWDs for identifying the two critical ground motions to be employed in the optimization process. The ISDR results of this initial stage were determined and presented in Fig. 11, for each of the 11 ground motions in comparison with their mean.

According to these results, the ground motion that gives the peak ISDR and the ground motion closest to the mean ISDR were selected to be employed in the optimization process. Thus, the analysis time for the optimization process has been significantly reduced. As seen in Fig. 11, the ground motion that gives the largest ISDR is "Tabas", where the ground motion that results the ISDR closest to the mean is the "Northridge" ground motion. The reason for selecting critical ground motions resulting the peak and mean ISDR values is based on the two limiting ISDR values as the constraints in the optimization, which was explained in detail in Section "Position Optimization Parameters."

7. Discussion of results

The optimum position and minimum number of VWDs of the prototype 15-story RC SMRF are determined with two metaheuristic search techniques of BA and DA. The convergence characteristics of the two search methods used are presented and compared with the so-called convergence curves. Then, the peak ISDR and floor acceleration demands are presented for the 2 selected ground motions. Besides, the analysis results of the 11 ground motions performed for the RC SMRF with optimally placed VWDs are investigated and the suitability of the selected 2 ground motions is demonstrated. Finally, the discussion is extended to the seismic responses of 15-story RC SMRF without VWD,

Table 2
Earthquake ground motion records used in the optimization process [53].

Earthquake	Date	Station	Mechanism	Mag (Mw)	Rjb (km)	Component	PGA (g)	PGV (cm/s)	PGD (cm)	Scale Factor
Düzce	1999	Bolu	Strike Slip	7.14	12.02	BOL090	0.806	65.9	13.1	1.2
Kocaeli	1999	Düzce	Strike Slip	7.51	13.6	DZC180	0.312	58.9	44.1	1.3
Superstititon	1987	Parachute Test Site	Strike Slip	6.54	0.95	PTS225	0.432	134.3	46.2	1.3
Kobe	1995	KJMA	Strike Slip	6.9	0.94	KJM000	0.821	81.3	17.7	1.3
San Fernando	1971	Pacoima Dam	Reverse	6.61	0	PUL164	1.226	112.5	35.4	1.0
Darfield	2010	GDLC	Strike Slip	7.0	1.2	GDLCN55W	0.765	116.1	100.4	1.1
N. Palm Springs	1986	North Palm Springs	Reverse Oblique	6.06	0	NPS210	0.595	73.2	11.5	1.1
Tabas	1978	9101 Tabas	Reverse	7.35	1.79	TAB-TR	0.861	123.4	93.6	1.3
Loma Priate	1989	16 LGPC	Reverse Oblique	6.93	0	LGP000	0.570	96.1	41.9	1.3
Erzincan	1992	95 Erzincan	Strike Slip	6.69	0	ERZ-EW	0.496	78.2	28.0	1.0
Northridge	1994	24,514 Sylmar OliveView Med FF	Reverse	6.69	1.74	SYL360	0.843	129.4	32.1	1.3

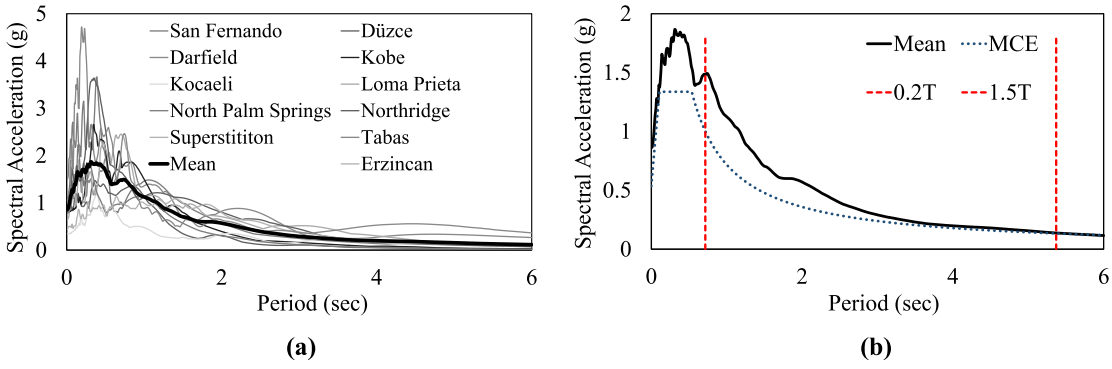

Fig. 7. (a) 5% damped acceleration response spectra and (b) the TBSC 2018-based design spectrum and the mean response spectrum of the selected ground motions.

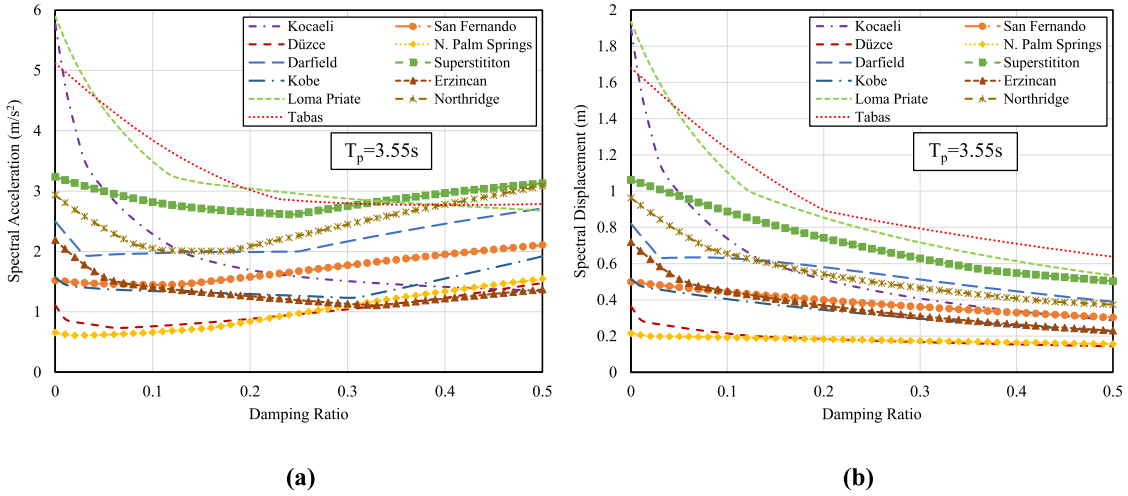

Fig. 8. Variation of (a) spectral acceleration and (b) spectral displacement with damping ratio for T_p = 3.55 s.

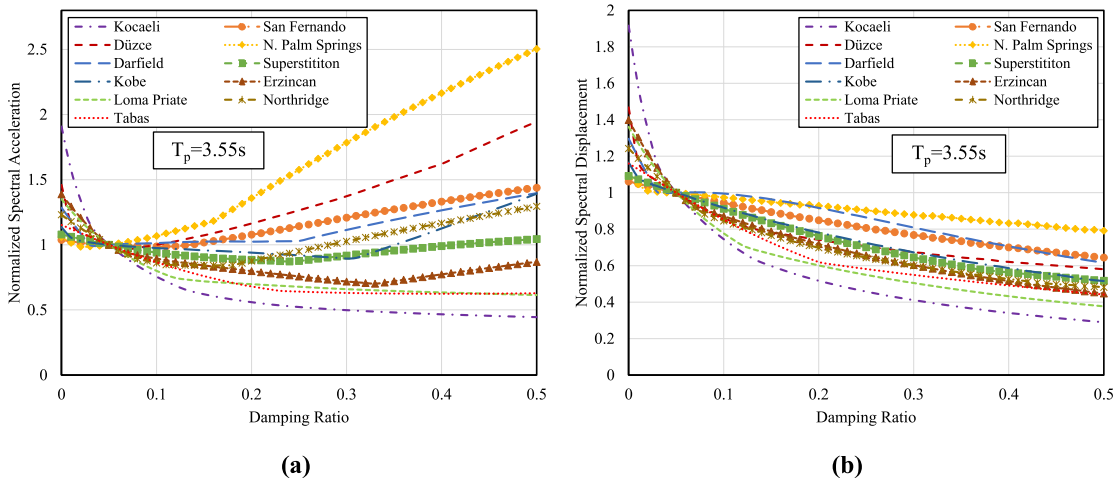

Fig. 9. Variation of (a) normalized spectral acceleration and (b) normalized spectral displacement with respect to 5% damping ratio.

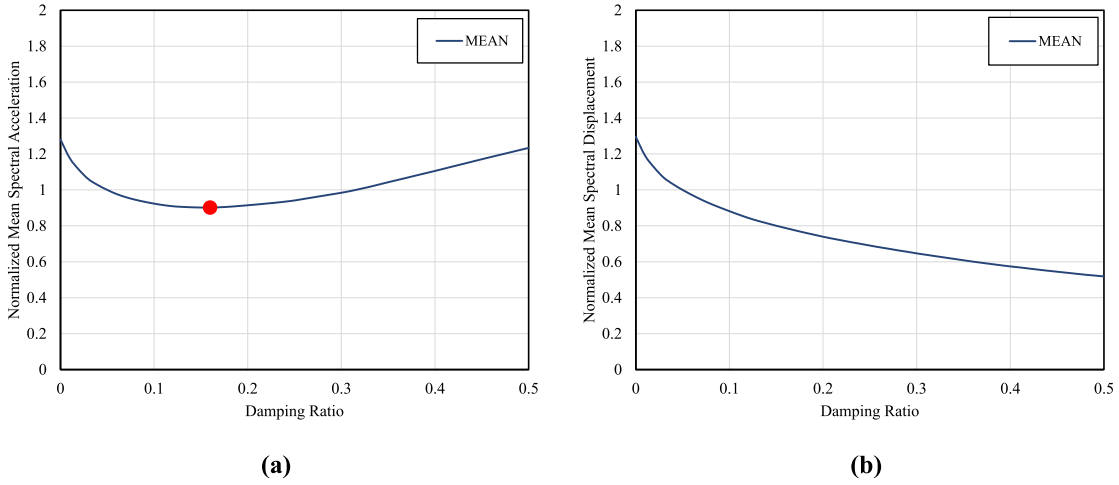

Fig. 10. Variation of (a) normalized mean spectral acceleration and (b) normalized mean spectral displacement with respect to 5% damping ratio.

with optimum VWD placement and full WVD placement in a comparative manner. The effects of the number and distribution of VWDs throughout the building for the structural response are examined.

7.1. Optimum VWD placement with BA and DA

The optimum number of VWDs and the corresponding distributions

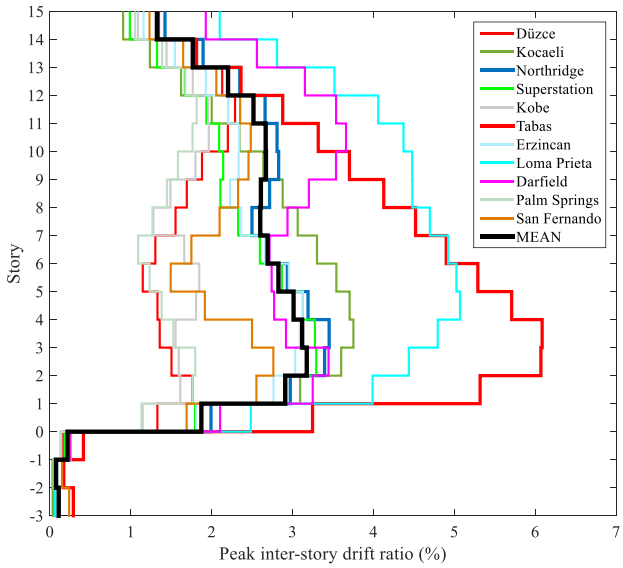

Fig. 11. Peak ISDR along the elevation of SMRF without VWD.

are computed based on the result of the optimization process through the NRHA using Tabas and Northridge ground motions. The optimum distribution of VWDs on one side of the structure determined by BA and DA is presented in Fig. 12. It should be noted that VWDs should be placed in the same bays on the opposite face of the building not to induce any torsional irregularity.

As shown in the optimum placement results of VWDs in Fig. 12, 19 and 20 VWDs were placed for only one side of the building by BA and DA, respectively, with the fulfillment of all the optimization constraints. Considering that the aim is to obtain the minimum number of VWDs by placing the VWDs in the most suitable spans in the proposed optimization method, BA has yield better results than DA. In addition, the spans identified for the VWD placement according to the optimum placement results found with BA and DA are similar. Since the peak ISDR demands generally concentrate at the 3rd, 4th and 5th stories as shown in the mean and maximum distributions for the peak ISDR in Fig. 11, both metaheuristic algorithms forced the optimization process to place the VWDs at these stories more than the others. Upper stories are not that effective in placing the VWDs when the VWD distribution of both algorithms are examined.

7.1.1. Convergence curves

The convergence histories showing the variation of the best solution in the most favorable run of the two algorithms (BA and DA) are plotted in Fig. 13. It should be noted that due to the random initialization of the algorithms, the initial values of the number of VWDs can differ from one algorithm to another for each case and this does not affect the optimization processes of the algorithms [54].

As it can be seen in Fig. 13, BA computed one less VWD on one side of the building compared to the DA. The BA reached the optimum number of VWD and corresponding positions much earlier than the DA. The horizontal base was reached after 28th iteration when BA applied, while DA showed a horizontal base after 85th iteration. These results show that the BA is more suitable to find the optimum position and minimum number of VWD for the proposed method and structural model.

7.2. Comparison of the building response depending on VWD installation

In this section, structural response of the RC SMRF building with optimum number of VWDs is compared to the cases of without any VWDs and with full VWD placement (placing the VWDs in all possible spans). Thus, the structural responses obtained in two extreme cases could be compared with the structural response obtained with optimum number of VWDs.

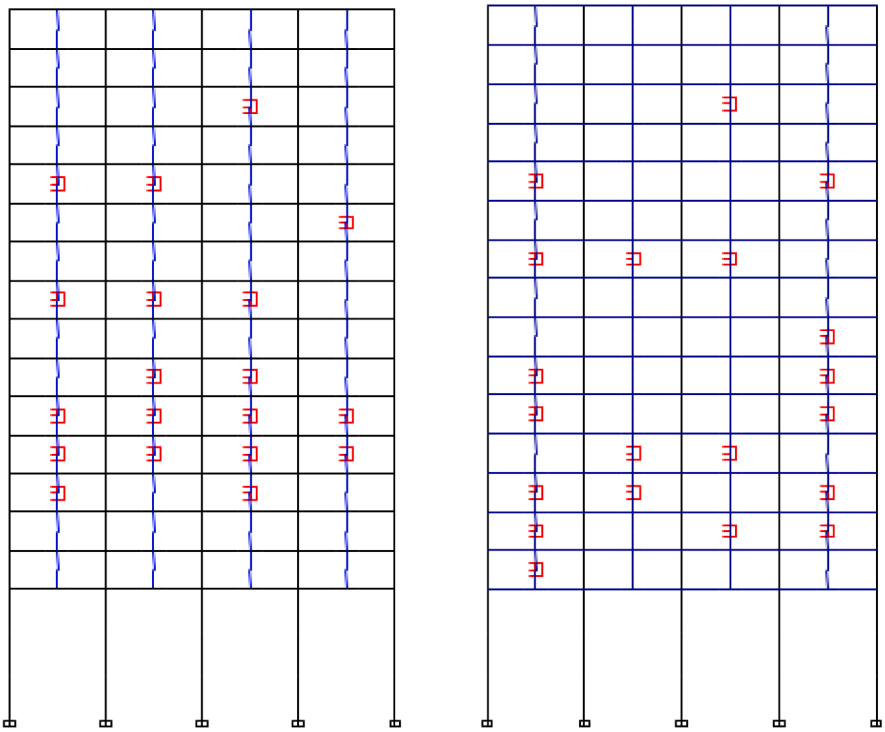

(a) BA (19 VWDs) **(b) DA (20 VWDs)**

Fig. 12. Optimum placement of VWDs on the building bays with (a) BA and (b) DA.

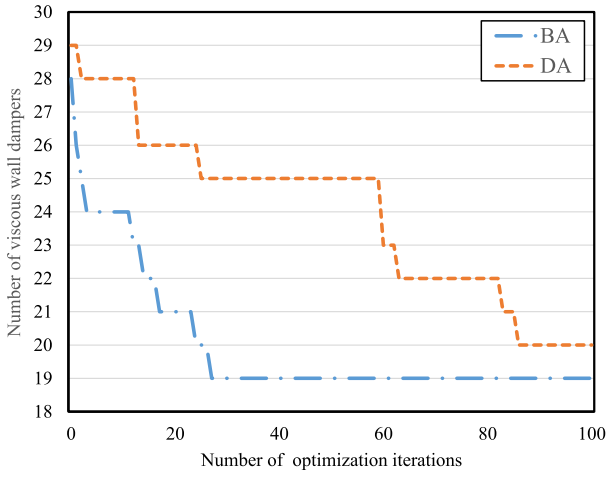

Fig. 13. Comparison of convergence curves for the best runs of BA and DA.

7.2.1. Comparisons of ISDRs

As previously mentioned, one of the main design criteria is the limitation of the ISDR response by setting the mean target as 3% or less, while the peak ISDR target is set as 4.5% or less from the NRHA results under the selected eleven ground motions. In this study, Tabas record represents the maximum ground motion and Northridge record represents the mean ground motion among the selected eleven ground motions. The ISDR of the RC SMRF optimized with BA and DA under the Tabas and Northridge ground motions along the building height are compared with the ISDR of the building without VWD and full span placement of VWDs as shown in Fig. 14.

Fig. 14 reveals that the peak ISDR target is achieved with a maximum value of 4.5% in the 4th story under Tabas record with the optimum VWD placement. The peak ISDR under Northridge record, which represents the mean of the ground motions, remained at 2.5% and did not exceed the limit value of 3% with the optimum VWD placement. On the other hand, when VWDs were not used, the peak ISDR values reached to 6% and 3.5% for Tabas and Northridge records, respectively. These ISDR demands are far beyond the code specified limiting values. Although it is not economically feasible when VWDs were placed in all spans, the ISDR demands were reduced significantly. This outcome is in good agreement with the variation of mean spectral displacement with respect to damping ratio. As the damping ratio increases, the spectral displacement reduces distinctively. These evaluations are valid for both of the RC SMRF optimizations by BA and DA, as ISDRs are quite close to each other for both cases. As expected, the distribution of VWDs in Fig. 12 by DA and BA is not that much different. Therefore, peak ISDR distribution under both earthquakes are close to each other. This proves the consistency and success in the application of the applied optimization process by utilizing two different optimization algorithms.

Although optimum VWD placement was made using only Tabas and Northridge earthquake records, the RC SMRF designed with optimum placement of VWDs was re-analyzed with the selected 11 earthquake records. The peak ISDRs and their mean as a result of 11 ground motion analyses results for the optimum VWD placement determined using BA and DA are presented in Fig. 15.

It is noted that the similar results presented in Figs. 14 and 15 justifies the use of only two ground motions, i.e. Tabas and Northridge, in the optimization analyses, for the sake of brevity. As can be seen in Fig. 15 for both of the considered optimization algorithms, the upper limit specified for the peak ISDR (4.5%) was not exceeded for any of the ground motions. Also, the mean of the peak ISDR of the selected 11 ground motion records is well below the specified mean ISDR limit (3%). Therefore, the selection of the two critical ground motion records (Tabas and Northridge records) in the optimization process is satisfactory in representing the selected eleven ground motion records. When the difference between the peak ISDR limit and the peak ISDR demand by Tabas record are compared with the difference between the mean ISDR limit and mean ISDR demand of 11 records, it is seen that the maximum ISDR limit controlled the results of the optimization process. Therefore, Tabas record dominates the overall optimization results when the ISDR is concerned.

7.2.2. Comparisons of floor accelerations

As mentioned before, one of the optimization constraints in this study is the floor accelerations. In the RC SMRF structure, floor accelerations must be minimized to satisfy the safety of building contents and comfort of the residents. The additional damping provided by the VWDs to the structural system is expected to reduce the floor accelerations as

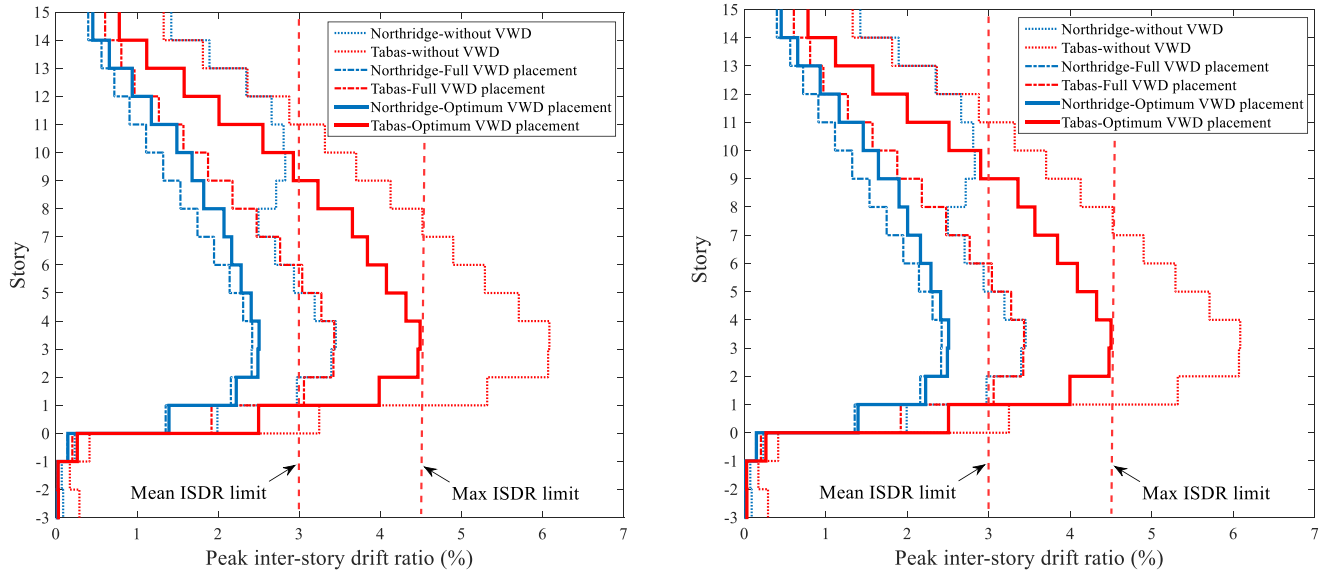

Fig. 14. ISDR along the height of RC SMRF without, full and optimum VWD placements by (a) BA and (b) DA.

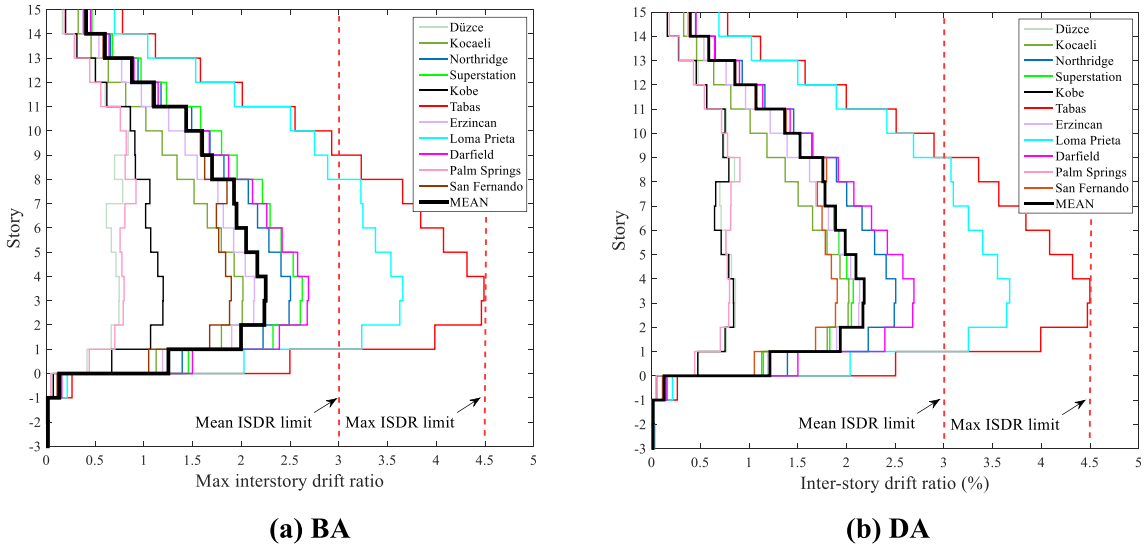

Fig. 15. The peak ISDRs and the mean ISDR along the height of RC SMRF designed with optimum VWD placements by (a) BA and (b) DA.

well. The change in floor accelerations with the use of VWDs is presented in this section. The peak floor accelerations of the RC SMRF optimized with BA and DA under the Tabas and Northridge ground motions are compared with the peak floor accelerations of the building without VWD and full span placement of VWDs as shown in Fig. 16. The limiting value of 10 m/s^2 is compared with the peak floor acceleration values obtained from the analyses results.

While the peak floor acceleration values computed in the building designed without VWD exceed 50 m/s^2 as shown in Fig. 16, the peak floor acceleration value for the optimum VWD placement by BA and DA achieved the specified limit. The peak floor acceleration values determined in the optimized building under the Tabas record are 9.8432 m/s^2 at 6th floor and 9.7768 m/s^2 at 5th floor for the BA and DA, respectively. In addition, for optimum VWD placement, the Northridge record resulted in peak floor acceleration of 9.4899 m/s^2 at 15th floor and 9.6877 m/s^2 at 15th floor for BA and DA, respectively. The presence of VWDs has reduced the peak floor accelerations considerably. On the other hand, the difference between the peak floor accelerations in the full span placed and optimum placed VWDs is not distinct. Conversely, the peak floor accelerations at the ground and roof stories of the building model with full span placed VWDs are greater than the ones for the building model with optimum placed VWDs. The difference between the results of the investigated algorithms is not distinct. For Tabas ground motion, the maximum difference between the results of BA and DA is 1.7 m/s^2 especially at the 8th floor, which is not the most critical floor in terms of peak floor accelerations. Therefore, both metaheuristic algorithms are considered to be effective in the optimization process.

The peak floor accelerations and their mean as a result of 11 ground motion analyses results for the optimum VWD placement determined using BA and DA are presented in Fig. 17.

According to Fig. 17, the peak value of the mean floor accelerations of the selected 11 earthquake records was determined as 7.1504 m/s^2 at the first floor and 7.1606 m/s^2 at the first floor for the BA and DA, respectively. Although the peak floor acceleration by the Tabas record used in the optimization process was calculated less than 10 m/s^2, the San Fernando earthquake record exceeds the peak floor acceleration value in the 1st floor with 11.3958 m/s^2 in Fig. 17a. Apart from the San Fernando earthquake record, it is seen that the optimization process was acceptable and the optimization process was shortened by selecting the representative mean earthquake and maximum earthquake records. The exceedance in the limiting peak floor acceleration by San Fernando record is 14%, which is considered to be acceptable in this study. However, the optimization can be repeated to satisfy the limiting value for each ground motion record. Due to the presence of one additional VWD in the first story by DA, the difference between the peak floor acceleration and the limit value is less for DA compared to the one for BA in the case of San Fernando record.

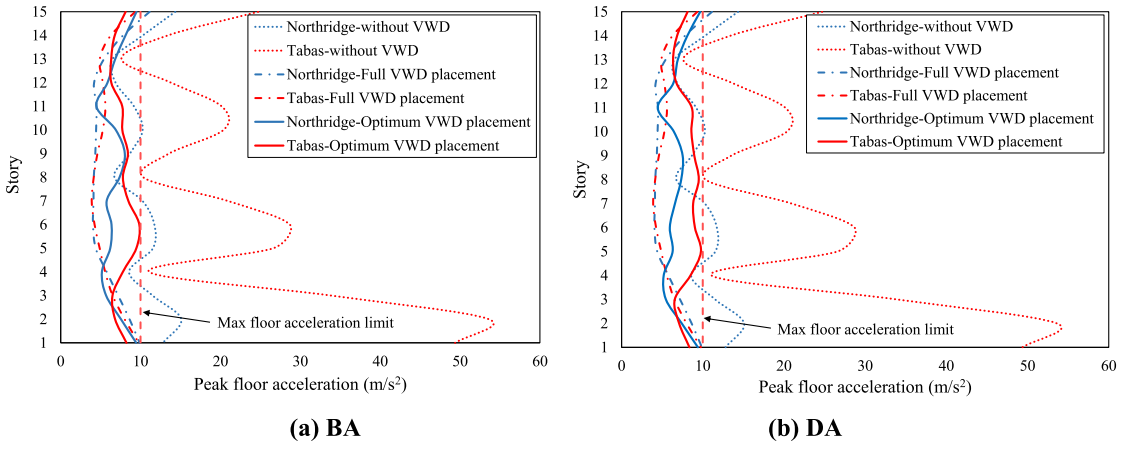

Fig. 16. Peak floor accelerations along the height of RC SMRF without, full and optimum VWD placements by (a) BA and (b) DA.

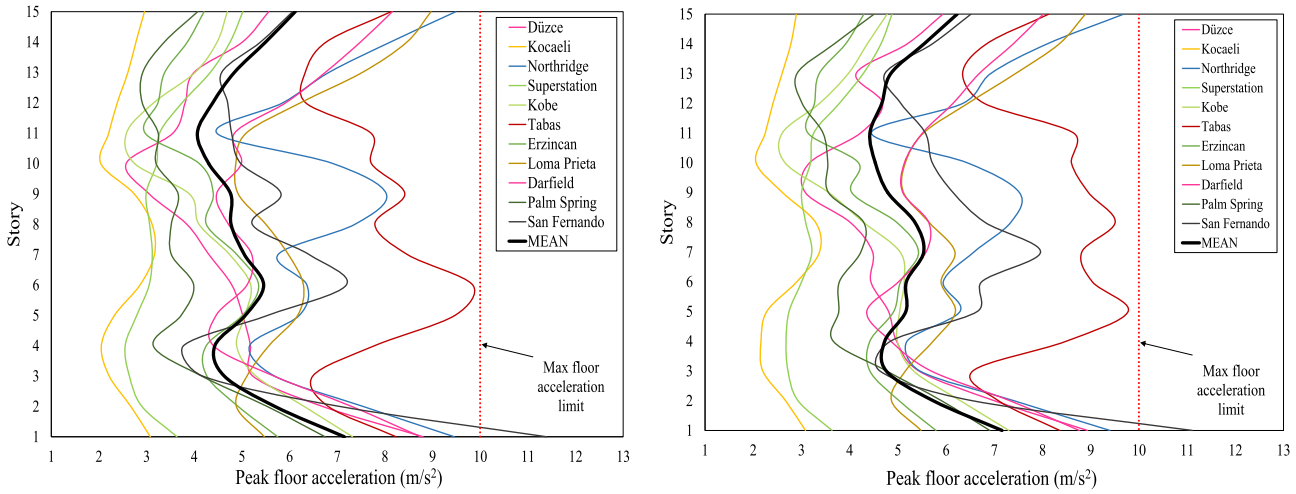

Fig. 17. The peak floor accelerations and their mean along the height of RC SMRF designed with optimum VWD placements by (a) BA and (b) DA.

7.2.3. Comparison of structural response

In this section, the general comparison of the peak structural response parameters is made for the cases without VWD, full VWD and optimized VWD distribution by BA and DA. The results of the maximum values of structural response parameters are given in Table 3.

As can be seen from Table 3, when the VWD is not placed in the structure, the floor acceleration value attains 53 m/s2 and the ISDR attains 6.00%. In most cases, Tabas record is the dominant ground motion record resulting in the most unfavorable structural response. However, when a total of 120 VWDs on both sides are placed in the structure, the critical ground motion record becomes the Northridge record as for the peak floor accelerations.

With the optimization using BA with 10 m/s2 floor acceleration limit and 4.50% ISDR limit, the ISDR was calculated as 4.49% for Tabas ground motion, which is very close to the upper limit. Similarly, the peak ISDR value is computed as 4.50% with DA.

If the VWDs are placed in all spans of the 15-story building, the difference in the peak floor accelerations recorded in the full VWD case and the optimum case are not significant. Particularly, the peak floor acceleration of the full VWD placed case is greater than the one for the building with optimum placed VWDs in the case of Northridge record. This increase in floor acceleration is thought to be caused by the increased damping with the use of more than necessary VWD. This outcome is in line with Fig. 10a, which indicates that the higher damping ratio does not mean reduced spectral accelerations. After a certain level of damping ratio, spectral accelerations increase. Therefore, it is important to determine the optimum number of VWDs and corresponding distribution to obtain the most effective structural responses. Otherwise, it is clearly seen from these results that undesirable structural performance especially in terms of floor accelerations can be encountered due to high damping supplied by the damper.

Table 3
The comparison of the peak structural responses of various cases.

VWD Placement Status	Number of VWD (including both sides of the structure)	Ground Motion Records	Peak floor acceleration (m/s^2)	Peak ISDR (%)
Without VWD	0	Northridge	15.09	3.45
		Tabas	53.60	6.08
All possible positions are full with VWD	120	Northridge	11.14	2.42
		Tabas	9.77	3.43
Optimal positions of VWD with BA	38	Northridge	9.49	2.50
		Tabas	9.84	4.49
Optimal positions of VWD with DA	40	Northridge	9.69	2.51
		Tabas	9.78	4.50

8. Summary and conclusions

In this study, two metaheuristic algorithms (BA and DA) were used for the position optimization of VWDs in a 15-story RC SMRF system. VWDs are the passive control devices that improves the structural response by providing additional damping capacity to the structures, reducing structural damages due to earthquake effects, especially in high-rise buildings. These elements are placed in the spans in the structures and dampen the earthquake effects between the floors. However, sensitivity in the placement of VWDs in the correct spans directly affects the seismic performance of the structural system. In addition, the number of damping elements used should be kept as low as possible for a cost effective design.

The scope of the study is to apply metaheuristic algorithms in the position optimization of VWDs in a RC SMRF to minimize the required number of VWDs without exceeding limits specified for the peak floor accelerations and ISDR. Bat Algorithm (BA) and Dragonfly Algorithm (DA) were employed to make the position optimization of VWDs under the selected and scaled 11 earthquake ground motion records. Following conclusions were drawn based on the results of this study:

1- BA and DA, which were used for position optimization in finding the minimum number of VWDs, remained within the specified peak floor acceleration and ISDR limits and managed to place the minimum number of VWDs in the most suitable spans.
2- BA resulted a slightly less number of VWDs compared to the results of DA. BA has placed 38 VWDs in 120 possible spans in both exterior faces of the building. While, DA has resulted 2 more VWDs compared to BA. In the optimization process, the dominant limiting criterion is controlled by the Tabas earthquake record with 4.50% ISDR limit.
3- Although BA and DA have started the optimization process with varying initial number of VWDs and their positions in the bays of the frame randomly, the minimum number of VWDs calculated by BA and DA has attained at the 28th and 85th iteration steps, respectively. Therefore, finding the optimum number of VWDs by

performing an optimization process is not only beneficial to achieve an improved structural response but also it allows making a cost effective design by minimizing the required number of VWDs. Although it is not convenient to compare the performance of two algorithms from the results of from a single optimization problem, in this study, BA reached one less VWD with a less number of optimization iterations.

4- The optimum positions of the VWDs determined by both algorithms are similar to each other. In both cases, the VWDs are generally placed in the lower stories. This is an expected outcome, when the ISDR profile is concerned along the elevation of the building. Since the peak ISDR demands are recorded in lower stories, VWDs are more effective with the increased relative displacement to provide additional damping to the system.

5- It has been evaluated that the use of VWDs with a number more than necessary can adversely affect the structural response, as in the case of Northridge record, which was resulted with higher peak floor accelerations when all the spans are full with VWDs compared to the optimum placed VWDs. Increased damping does not always result in a better structural response particularly in terms of floor accelerations. Therefore, finding the optimum number of VWDs by performing an optimization process is not only beneficial to achieve an improved structural response but also it allows making a cost effective design by minimizing the required number of VWDs.

CRediT authorship contribution statement

Ali Erdem Çerçevik: Methodology, Investigation, Software, Writing–original draft. **Özgür Avşar:** Conceptualization, Investigation, Writing–original draft, Writing – review & editing. **Abdullah Dilsiz:** Methodology, Resources, Writing – review & editing.

Declaration of Competing Interest

The authors declare that they have no known competing financial interests or personal relationships that could have appeared to influence the work reported in this paper.

References

[1] Dilsiz A, Mohammed M, Özuygur AR, Mohamed M. Seismic Design and Performance of Reinforced Concrete Special Moment Resisting Frames with Wall Dampers. J Earthquake Eng 2020. https://doi.org/10.1080/13632469.2019.1692741.

[2] Arima F, Miyasaki M, Tanaka H, Yamasaki Y. A study on building with large damping using viscous damping walls. Ninth World Conference on Earthquake Engineering, 1988.

[3] Newell J, Love J, Sinclair M, Chen YN, Kasalanati A. Seismic design of a 15 story hospital using viscous wall dampers. In: Structures Congress 2011 - Proceedings of the 2011 Structures Congress; 2011. https://doi.org/10.1061/41171(401)72.

[4] ASCE. Minimum Design Loads for Buildings and Other Structures 2005.

[5] Lu X, Zhou Y, Yan F. Shaking table test and numerical analysis of RC frames with viscous wall dampers. J Struct Eng 2008;134(1):64–76. https://doi.org/10.1061/(ASCE)0733-9445(2008)134:1(64).

[6] Zhou Y, Chen P, Zhang D, Gong S, Lu W. A new analytical model for viscous wall dampers and its experimental validation. Eng Struct 2018;163:224–40. https://doi.org/10.1016/j.engstruct.2018.02.049.

[7] Hejazi F, Shoaei MD, Tousi A, Jaafar MS. Analytical Model for Viscous Wall Dampers. Comput-Aided Civ Infrastruct Eng 2016;31(5):381–99. https://doi.org/10.1111/mice:2016.31.issue-510.1111/mice:12161.

[8] Murakami Y, Noshi K, Fujita K, Tsuji M, Takewaki I. Optimal placement of hysteretic dampers via adaptive sensitivity-smoothing algorithm. Computational Methods in Applied Sciences 2015. https://doi.org/10.1007/978-3-319-18320-6_13.

[9] Takewaki I. Optimal damper placement for minimum transfer functions. Earthquake Eng Struct Dyn 1997. https://doi.org/10.1002/(SICI)1096-9845(199711)26:11<1113::AID-EQE696>3.0.CO;2-X.

[10] Kanno Y. Damper placement optimization in a shear building model with discrete design variables: A mixed-integer second-order cone programming approach. Earthquake Eng Struct Dyn 2013;42(11):1657–76. https://doi.org/10.1002/eqe.v42.1110.1002/eqe.2292.

[11] Wu B, Ou J-P, Soong TT. Optimal placement of energy dissipation devices for three-dimensional structures. Eng Struct 1997;19(2):113–25. https://doi.org/10.1016/S0141-0296(96)00034-X.

[12] Kondo K, Takewaki I. Simultaneous Approach to Critical Fault Rupture Slip Distribution and Optimal Damper Placement for Resilient Building Design. Frontiers in Built Environment 2019. https://doi.org/10.3389/fbuil.2019.00126.

[13] Bogdanovic A, Rakicevic Z. Optimal damper placement using combined fitness function. Frontiers in Built Environment 2019. https://doi.org/10.3389/fbuil.2019.00004.

[14] Mousavi SA, Ghorbani-Tanha AK. Optimum placement and characteristics of velocity-dependent dampers under seismic excitation. Journal of Earthquake Engineering and Engineering Vibration 2012;11(3):403–14. https://doi.org/10.1007/s11803-012-0130-4.

[15] Ok SY, Song J, Park KS. Optimal design of hysteretic dampers connecting adjacent structures using multi-objective genetic algorithm and stochastic linearization method. Eng Struct 2008;30(5):1240–9. https://doi.org/10.1016/j.engstruct.2007.07.019.

[16] Su C, Li B, Chen T, Dai X. Stochastic optimal design of nonlinear viscous dampers for large-scale structures subjected to non-stationary seismic excitations based on dimension-reduced explicit method. Eng Struct 2018;175:217–30. https://doi.org/10.1016/j.engstruct.2018.08.028.

[17] Roger G. Integrated Design of Damper Placement and Parameters for Passive Control of Randomly Base-Excited Structures. 15th World Conference on Earthquake Engineering (15WCEE). 2012.

[18] Park KS, Koh HM, Hahm D. Integrated optimum design of viscoelastically damped structural systems. Eng Struct 2004;26(5):581–91. https://doi.org/10.1016/j.engstruct.2003.12.004.

[19] Gandomi AH, Yang XS, Talatahari S, Alavi AH. Metaheuristic Applications in Structures and Infrastructures. 2013. https://doi.org/10.1016/C2011-0-08778-1.

[20] Fujita K, Moustafa A, Takewaki I. Optimal placement of viscoelastic dampers and supporting members under variable critical excitations. Earthquake and Structures 2010;1(1):43–67. https://doi.org/10.12989/eas.2010.1.1.043.

[21] Movaffaghi H, Friberg O. Optimal placement of dampers in structures using genetic algorithm. Engineering Computations (Swansea, Wales) 2006;23(6):597–606. https://doi.org/10.1108/02644400610680324.

[22] Warsito B, Yasin H, Prahutama A. Particle swarm optimization versus gradient based methods in optimizing neural network. J Phys Conf Ser 2019;1217:012101. https://doi.org/10.1088/1742-6596/1217/1/012101.

[23] Sonmez M, Aydin E, Karabork T. Using an artificial bee colony algorithm for the optimal placement of viscous dampers in planar building frames. Struct Multidiscip Optim 2013;48(2):395–409. https://doi.org/10.1007/s00158-013-0892-y.

[24] Cetin H, Aydin E, Ozturk B. Optimal design and distribution of viscous dampers for shear building structures under seismic excitations. Frontiers in Built Environment 2019. https://doi.org/10.3389/fbuil.2019.00090.

[25] Bishop JA, Striz AG. On using genetic algorithms for optimum damper placement in space trusses. Struct Multidiscip Optim 2004;28(2-3). https://doi.org/10.1007/s00158-004-0441-9.

[26] Sarcheshmehpour M, Estekanchi HE, Ghannad MA. Optimum placement of supplementary viscous dampers for seismic rehabilitation of steel frames considering soil–structure interaction. Struct Des Tall Special Build 2020;29(1). https://doi.org/10.1002/tal.v29.110.1002/tal.1682.

[27] Miguel LFF, Fadel Miguel LF, Lopez RH. A firefly algorithm for the design of force and placement of friction dampers for control of man-induced vibrations in footbridges. Optimization and Engineering 2015;16(3):633–61. https://doi.org/10.1007/s11081-014-9269-3.

[28] Yang XS. A new metaheuristic Bat-inspired Algorithm. Studies in Computational Intelligence, vol. 284, 2010. DOI: 10.1007/978-3-642-12538-6_6.

[29] Mirjalili S. Dragonfly algorithm: a new meta-heuristic optimization technique for solving single-objective, discrete, and multi-objective problems. Neural Comput Appl 2016;27(4):1053–73. https://doi.org/10.1007/s00521-015-1920-1.

[30] Nakamura RYM, Pereira LAM, Rodrigues D, Costa KAP, Papa JP, Yang X-S. In: Swarm Intelligence and Bio-Inspired Computation. Elsevier; 2013. p. 225–37. https://doi.org/10.1016/B978-0-12-405163-8.00009-0.

[31] Mafarja MM, Eleyan D, Jaber I, Hammouri A, Mirjalili S. Binary Dragonfly Algorithm for Feature Selection. Proceedings - 2017 International Conference on New Trends in Computing Sciences, ICTCS 2017, vol. 2018- Janua, 2017. DOI: 10.1109/ICTCS.2017.43.

[32] Gupta D, Arora J, Agrawal U, Khanna A, de Albuquerque VHC. Optimized Binary Bat algorithm for classification of white blood cells. Measurement: Journal of the International Measurement Confederation 2019;143:180–90. https://doi.org/10.1016/j.measurement.2019.01.002.

[33] Kizilkaya B, Caglar M, Al-Turjman F, Ever E. Binary search tree based hierarchical placement algorithm for IoT based smart parking applications. Internet of Things 2019;5:71–83. https://doi.org/10.1016/j.iot.2018.12.001.

[34] Sahu PC, Sahoo S, Prusty RC, Sahu BK. Binary Dragonfly Algorithm-Designed Fuzzy Cascade Controller for AGC of Multi-area Power System with Nonlinearities. Lecture Notes in Networks and Systems, vol. 151, 2021. DOI: 10.1007/978-981-15-8218-9_37.

[35] Too J, Mirjalili S. A Hyper Learning Binary Dragonfly Algorithm for Feature Selection: A COVID-19 Case Study. Knowl-Based Syst 2021;212:106553. https://doi.org/10.1016/j.knosys.2020.106553.

[36] ETABS. Integrated Building Design Software, Computers and Structures, Inc: Berkeley, California. 2018.

[37] Kaveh A, Zakian P. Optimal design of steel frames under seismic loading using two meta-heuristic algorithms. J Constr Steel Res 2013;82:111–30. https://doi.org/10.1016/j.jcsr.2012.12.003.

[38] Hasançebi O, Teke T, Pekcan O. A bat-inspired algorithm for structural optimization. Comput Struct 2013;128:77–90. https://doi.org/10.1016/j.compstruc.2013.07.006.

[39] Osaba E, Yang X-S, Diaz F, Lopez-Garcia P, Carballedo R. An improved discrete bat algorithm for symmetric and asymmetric Traveling Salesman Problems. Eng Appl Artif Intell 2016;48:59–71. https://doi.org/10.1016/j.engappai.2015.10.006.
[40] Tsai PW, Nguyen TT, Dao TK. Robot path planning optimization based on multiobjective grey wolf optimizer 2017;vol. 536. https://doi.org/10.1007/978-3-319-48490-7_20.
[41] Fister I, Rauter S, Yang X-S, Ljubič K, Fister I. Planning the sports training sessions with the bat algorithm. Neurocomputing 2015;149:993–1002. https://doi.org/10.1016/j.neucom.2014.07.034.
[42] Kaveh A, Zakian P. Enhanced bat algorithm for optimal design of skeletal structures. *Asian.* Journal of Civil Engineering 2014.
[43] Yuan Y, Lv L, Wang X, Song X. Optimization of a frame structure using the Coulomb force search strategy-based dragonfly algorithm. Eng Optim 2020;52(6):915–31. https://doi.org/10.1080/0305215X.2019.1618290.
[44] Yıldız BS, Yıldız AR. The Harris hawks optimization algorithm, salp swarm algorithm, grasshopper optimization algorithm and dragonfly algorithm for structural design optimization of vehicle components. Materialpruefung/Materials Testing 2019. DOI: 10.3139/120.111379.
[45] Mafarja M, Aljarah I, Heidari AA, Faris H, Fournier-Viger P, Li X, et al. Binary dragonfly optimization for feature selection using time-varying transfer functions. Knowl-Based Syst 2018;161:185–204. https://doi.org/10.1016/j.knosys.2018.08.003.
[46] Jafari M, Bayati Chaleshtari MH. Using dragonfly algorithm for optimization of orthotropic infinite plates with a quasi-triangular cut-out. European Journal of Mechanics, A/Solids 2017;66:1–14. https://doi.org/10.1016/j.euromechsol.2017.06.003.
[47] TBSC. Turkish building seismic code, disaster and emergency management presidency. Ankara: Republic of Turkey Prime Ministry. 2018.
[48] Building-specific GSKV. earthquake damage estimation. Ph.D. dissertation. Department of Civil and Civil and Environmental Engineering. Stanford University; 1993.
[49] Elenas A, Meskouris K. Correlation study between seismic acceleration parameters and damage indices of structures. Eng Struct 2001;23(6):698–704. https://doi.org/10.1016/S0141-0296(00)00074-2.
[50] Lagaros ND, Mitropoulou CC. The effect of uncertainties in seismic loss estimation of steel and reinforced concrete composite buildings. Struct Infrastruct Eng 2013;9(6):546–66. https://doi.org/10.1080/15732479.2011.593527.
[51] Dynamic Isolation Systems I. Viscous wall damper modeling guide. McCarran, NV: Dynamic Isolation Systems Inc. 2017.
[52] Scheller J, Constantinou MC, Hall K. Response History Analysis of Structures with Seismic Isolation and Energy Dissipation Systems : Verification Examples for Program SAP2000 by Mceer 1999:14260–300.
[53] PEER. Ground Motion Database. Shallow Crustal Earthquakes in Active Tectonic Regimes, NGA-West2 2019. http://ngawest2.berkeley.edu/.
[54] Kazimipour B, Li X, Qin AK. A review of population initialization techniques for evolutionary algorithms. In: Proceedings of the 2014 IEEE Congress on Evolutionary Computation; 2014, 2014.. https://doi.org/10.1109/CEC.2014.6900618.
[55] Providakis CP. Effect of supplemental damping on LRB and FPS seismic isolators under near-fault ground motions. Soil Dynamics and Earthquake Engineering 2009;29(1):80–90. https://doi.org/10.1016/j.soildyn.2008.01.012.
[56] Çerçevik AE, Avşar Ö, Hasançebi O. Optimum design of seismic isolation systems using metaheuristic search methods. Soil Dynamics and Earthquake Engineering 2020;131:106012. https://doi.org/10.1016/j.soildyn.2019.106012.